Article

Discovery Medicine 2024; 36(187): 1721–1731
https://doi.org/10.24976/Discov.Med.202436187.158

Simvastatin Inhibits the Formation of NETs by the Mac-1 Pathway to Reduce Hepatic Ischemia-Reperfusion Injury under High-Fat Conditions

Shikai Wang[1], Zhipeng Li[1], Yunxiang Chang[1], Kai Dong[1], Di He[1], Xinsheng Cheng[1,*]

[1]Department of Hepatobiliary and Pancreatic Surgery, Union Shenzhen Hospital, Huazhong University of Science and Technology, 518056 Shenzhen, Guangdong, China

*Correspondence: shenzhenhos_21@sina.com (Xinsheng Cheng)

Published: 20 August 2024

Background: Hyperlipidemia is one of the main causes of aggravated hepatic ischemia-reperfusion injury (IRI). Simvastatin (SIM), a lipid-lowering drug, has been shown to effectively alleviate IRI caused by hyperlipidemia. However, the regulatory mechanism by which SIM alleviates hyperlipidemia-induced hepatic IRI is still not clear. This study aims to explore the potential mechanisms of SIM in inhibiting hyperlipidemia-induced hepatic IRI, providing new therapeutic strategies for the alleviation of hepatic IRI.

Methods: An animal model of hyperlipidemia was induced by feeding mice a high-fat diet for 8 weeks. Subsequently, a hepatic IRI animal model of hyperlipidemia was established by occluding the hepatic artery and portal vein for one hour, followed by reperfusion for 6 or 12 h. Enzyme linked immunosorbent assay, Western blotting, hematoxylin-eosin (H&E) staining, immunohistochemistry, immunofluorescence, and Terminal-deoxynucleoitidyl Transferase Mediated Nick End Labeling assay, were used to evaluate liver injury, neutrophil extracellular traps (NETs) formation, and related molecular mechanisms.

Results: Hepatic IRI was accelerated by hyperlipidemia, which enhanced the expression of oxidized low-density lipoprotein (oxLDL) and Macrophage-1antigen (Mac-1), leading to the promotion of NETs formation and apoptosis of liver cells. The administration of simvastatin reduced the levels of oxLDL and Mac-1, decreased the formation of NETs, and alleviated hepatic IRI induced by hyperlipidemia.

Conclusions: Simvastatin reduced hyperlipidemia-induced hepatic IRI by inhibiting the formation of NETs through the regulation of the oxLDL/Mac-1 pathway.

Keywords: hyperlipidemia; neutrophil extracellular traps (NETs); simvastatin; hepatic ischemia reperfusion injury

---

Introduction

Hepatic ischemia-reperfusion injury (IRI) is a significant contributor to postoperative complications and mortality in liver diseases [1]. The transition from ischemia to reperfusion is a key pathological process leading to hepatic damage [2]. During the reperfusion injury phase, immune cells are widely activated, triggering a series of sterile inflammatory reactions, ultimately resulting in hepatic function damage or even death [3]. Despite extensive research, the occurrence and development mechanisms of hepatic IRI remain unclear.

In recent decades, the prevalence of hyperlipidemia due to a high-fat diet has been increasing, leading to its significant role in inducing hepatic IRI [4]. Tung *et al.* [5] have demonstrated that hyperlipidemia can result in hepatic lipid accumulation, elevate levels of serum alanine aminotransferase (ALT) and aspartate aminotransferase (AST), induce hepatocyte apoptosis, and accelerate hepatic tissue necrosis in rats. In addition, hyperlipidemic patients exhibit high levels of low-density lipoprotein (LDL) and triglycerides, and during IRI, a substantial amount of LDL is oxidized into oxidized low-density lipoprotein (oxLDL) [6]. Platelets stimulated by oxLDL enhance the pathological accumulation of immune cell subsets and neutrophils through cellular interactions [7]. Neutrophils, as the most abundant and rapid-reacting immune cells in the blood, aggregate and activate in large numbers during IRI [8], releasing a three-dimensional network structure composed of DNA called neutrophil extracellular traps (NETs) [9]. These NETs are known to damage vascular endothelium, activate the inflammation-coagulation cascade, and worsen microcirculatory damage [10,11]. While some studies have demonstrated that the formation of NETs depends on reactive oxygen species (ROS) and nicotinamide adenine dinucleotide phosphate (NADPH) oxidase [12], the communication factors that regulate NETs formation between cells have not been fully elucidated. Macrophage-1 antigen (Mac-1, CD11b/CD18), the most abundant and important $\beta2$ integrin on the surface of neutrophils, can promote neutrophil adhesion and recruitment to inflammatory sites by crossing endothelial cells [13]. Recent studies have shown that Mac-1 participates in the formation of NETs. Behnen *et al*. [14] found that Mac-1 was involved in FcγRIIIb-mediated NETs generation. After applying Mac-1 antibodies, NETs formation significantly decreased. However, it has not been reported whether oxLDL affects hepatic IRI by regulating the specific membrane receptor Mac-1 expression on polymorphonuclear leukocytes and stimulating the production of NETs.

Simvastatin (SIM) is a commonly used lipid-lowering statin in clinical practice. In recent years, it has shown efficacy in treating IRI such as hepatic [15], myocardial [16], and intestinal IRI [17]. However, the protective mechanism of SIM in IRI has not been fully elucidated. Cowled *et al*. [18] have indicated that SIM can inhibit neutrophil infiltration induced by IRI. It is speculated that the protective effect of SIM on hepatic IRI may depend on the inhibition of NETs formation, thereby alleviating the mechanism of liver functional damage. This study aims to investigate whether SIM can reduce hyperlipidemia-induced hepatic IRI by regulating the oxLDL/Mac1 pathway to inhibit NETs formation.

Materials and Methods

Establishment of the Hepatic IRI Model Caused by Hyperlipidemia

A total of 60 male C57BL/6 mice, ten weeks old and weighing 26 ± 1.7 g, were purchased from Guangzhou Ruige Biological Technology Co., Ltd. The mice were used to model hyperlipidemia, following a protocol from previous study [19], where they were fed a high-fat diet (XTHF60, Jiangsu Xietong Pharmaceutical Bio-engineering Co., Jiangsu, China). The remaining feed and water intake were measured daily to calculate the previous day's consumption. The bedding was changed every 4 days, and the mice were weighed in each group. The modeling period lasted 8 weeks. All animal breeding and other experimental procedures complied with relevant management guidelines and ethical requirements for experimental animals.

To establish the hepatic IRI model, mice were fasted for 12 h before modeling but were allowed access to water. The model was based on previous reports [20]. Specifically, mice were intraperitoneally injected with pentobarbital sodium (80 mg/kg) for anesthesia. A midline longitudinal incision was made in the abdomen to expose the hepatic cavity, and the specific locations of the left and median lobes of the liver were identified. Microvascular clamps (1011032, Shanghai Medical Instruments Co., Ltd., Shanghai, China) were used to occlude the hepatic artery and portal vein for 1 h, resulting in ischemia of the left and middle lobes of the liver. During this time, visible color changes indicating ischemic hepatic lobes were observed. After confirming successful blood flow obstruction, the abdominal cavity was temporarily closed, the incision in the abdominal wall was covered, and the vascular clip was released after the predetermined ischemic period. Finally, the abdomen was closed. In the sham-operated group, mice underwent the same surgical procedure but without occlusion of the hepatic veins. Subsequently, mice were sacrificed with cervical dislocation method at 6 and 12 h after reperfusion, and liver and serum samples were immediately collected for further analysis. The animal experiments were performed following the Animals (Scientific Procedures) Act 1986 and approved by the Animal Care Committee of Guangzhou Seyotin Biotechnology Co., Ltd. (SYT2023010).

Animal Grouping and Intervention

The mice were divided into four groups: the control group, the 6-hour hepatic IRI group, the 12-hour hepatic IRI group, and the 12-hour hepatic IRI + SIM group (IRI 12 h + SIM), with 10 mice in each group. In the IRI 12 h + SIM group, the mice were simultaneously administered SIM (S129538, Aladdin, Shanghai, China) at a dosage of 5 mg/kg through intraperitoneal injection during the induction of ischemia [20]. The remaining two groups received an intraperitoneal injection of saline. Additionally, 20 hyperlipidemia mice were randomly assigned to the IRI 12 h + SIM + oe-Mac-1 group, IRI 12 h + SIM + oe-NC group, IRI 12 h + si-Mac-1 group, and IRI 12 h + si-NC group, with 5 mice in each group. Three days before the IR operations, they were respectively infected with Viruses (8.87×10^{13} vg/mL) pAV-CMV-Mac-1-P2A-GFP (HY22839, WZ Biosciences, Jinan, Shandong, China), pAV-CMV-P2A-GFP, pAV-4in1-shMac-1-GFP (HY23619, WZ Biosciences, Shandong, China), and pAV-4in1-shNC-GFP by intravenous injection (40 µL/mouse). The Adeno-associated virus (AAV8) containing Mac-1 was obtained from WZ Biosciences (Shandong, China). The sequences related to Mac-1 synthesis are shown in **Supplementary Table 1**.

Biochemical Index Assays

Blood samples from mice were collected and allowed to stand for 30 min. Subsequently, the samples were centrifuged at 3500 rpm for 10 min to separate the serum. The levels of ALT and AST in the serum were determined using an automatic biochemical analyzer (Iqlaahgabdfaazm-blt, Thermo Fisher Scientific, Waltham, MA, USA). The concentrations of oxLDL (ab285269, Beyotime, Shanghai, China), Tumor necrosis factor-α (PT516, Beyotime, Shanghai, China), and Interleukin-6 (PI330, Beyotime, Shanghai, China) in the serum were analyzed using Enzyme linked immunosorbent assay kits. Additionally, NETs-associated myeloperoxidase (MPO)-DNA complexes were quantified using the Cell Death ELISA kit (MA549071, Thermo Fisher Scientific, USA).

Hematoxylin-Eosin (H&E) Staining

Mice hepatic tissues were fixed in a 4% paraformaldehyde solution (BL539A, Biosharp, Beijing, China), dehydrated using various concentrations of ethanol, and then subjected to xylene transparency, paraffin embedding, sectioning, dewaxing, rehydration, and hematoxylin-eosin staining (C0105M, Beyotime, Shanghai, China). The resulting pathological changes in hepatic tissue were observed under a light microscope (MS60, Mshot, Guangzhou Mshot Photoelectric Technology CO., Ltd., Guangzhou, China).

TUNEL Assay

The paraffin sections were stained according to the instructions of the Terminal-deoxynucleoitidyl Transferase Mediated Nick End Labeling apoptosis detection kit (C1088, Beyotime, Shanghai, China). Randomly selected fields were observed under a high-power microscope (CKX53, Olympus, Tokyo, Japan), and 5 fields were counted on each slide to calculate the average number of total liver cells and TUNEL-positive cells.

Immunofluorescence Staining

As described in 2.5, hepatic tissues from mice were fixed in a 4% paraformaldehyde solution (BL539A, Biosharp, Beijing, China), dehydrated using various ethanol concentrations, and then subjected to xylene transparency, paraffin embedding, sectioning, dewaxing, and rehydration. Subsequently, these hepatic tissues were incubated overnight at 4 °C with antibodies against citrullinated histone H3 (Cit-H3) (EPR20358120, Abcam, Shanghai, China), MPO (ab45977, Abcam, Shanghai, China), and Mac-1 (EPR19900147, Abcam, Shanghai, China). The secondary antibodies were then incubated at room temperature on a shaking bed for 1 h. 4′,6-diamidino-2-phenylindole (STC448, Seyotin, Guangzhou, China) was used for DNA staining. The sections were observed and imaged under a fluorescence microscope (CKX53, Olympus, Tokyo, Japan). The ImageJ software (V1.8.0.112, Rawak Software Inc., Stuttgart, Germany) was used to analyze these results.

Western Blotting

Proteins were extracted from the hepatic tissues of mice and quantitatively analyzed using BCA kits (P0012, Beyotime, Shanghai, China). Subsequently, 10 µL of protein samples from each group were subjected to Sodium Dodecyl Sulfate-Polyacrylamide Gel Electrophoresis (SDS-PAGE), followed by transfer and blocking. Primary antibodies including Cleaved Caspase-3 (C-Caspase3) (1/1000, ab2302, Abcam, Shanghai, China), Caspase-3 (1/10000, ab32042, Abcam, Shanghai, China), BCL2-Associated X (1/500, ab182733, Abcam, Shanghai, China), B-cell lymphoma-2 (1/2000, ab182858, Abcam, Shanghai, China), Cit-H3 (1/5000, ab219407, Abcam, Shanghai, China), p65 (1/2000, ab32536, Abcam, Shanghai, China), phospho-nuclear factor kappa-B/p65 (1/500, ab53489, Abcam, Shanghai, China), Mac-1 (1/1000, Abcam, Shanghai, China), and GAPDH (1/5000, ab8245, Abcam, Shanghai, China) were incubated. This was followed by the incubation with secondary antibodies including C-Caspase3 (1/1000, ab2302, Abcam, Shanghai, China), Caspase-3 (1/10000, ab216777, Abcam, Shanghai, China), Bax (1/10000, ab216776, Abcam, Shanghai, China), Bcl-2 (1/10000, ab32124, Abcam, Shanghai, China), Cit-H3 (1/10000, ab97051, Abcam, Shanghai, China), p65 (1/10000, ab216776, Abcam, Shanghai, China), p-p65 (1/10000, ab43041, Abcam, Shanghai, China), Mac-1 (1/10000, Abcam, Shanghai, China), and GAPDH (1/10000, ab8245, Abcam, Shanghai, China) on a shaking bed at room temperature for 1 h. The enhanced chemiluminescence luminescent solution (PK10003, Proteintech, Wuhan, China) was used for exposure, and ImageJ (V1.8.0.112, Rawak Software Inc., Stuttgart, Germany) software was used for band statistical analysis.

Statistical Analysis

All experimental results were replicated three times. The experimental data are represented as mean ± standard deviation (SD). Statistical analysis was conducted using GraphPad Prism 6 software (GraphPad Software Inc., San Diego, CA, USA). Differences were assessed using the Student's t-test for two groups or one-way Analysis of Variance for more than two groups. Statistical significance was considered when the p-value was less than 0.05.

Results

Hyperlipidemia Enhanced Hepatic IRI

To investigate the impact of hyperlipidemia on hepatic IRI, we fed mice a high-fat diet for 8 weeks to induce hyperlipidemia. Subsequently, we subjected the hyperlipidemic mice to hepatic IRI by occluding the hepatic artery and portal vein for 1 h. To assess the severity of liver function damage and its association with the duration of IRI, we randomly divided the mice into three groups: the control group, the 6-hour group, and the 12-hour group, based on the reperfusion time. The results showed a significant increase in ALT (Fig. 1A, $p < 0.05$) and AST (Fig. 1A, $p < 0.01$) levels at 6 and 12 h after reperfusion, compared with the control group (Fig. 1A). Furthermore, we conducted a histopathological examination of hepatic samples, revealing a significant aggravation of hepatic tissue damage at 6 and 12 h after reperfusion, as evidenced by the increased area of coagulative necrosis in HE-stained sections (Fig. 1B). The hepatic cord disappeared in hepatic tissue, and a significant increase in the area of hepatic tissue coagulation necrosis was observed (indicated by black arrows). Meanwhile, the number of apoptotic cells in the liver of hyperlipidemic mice was observed to increase as the reper-

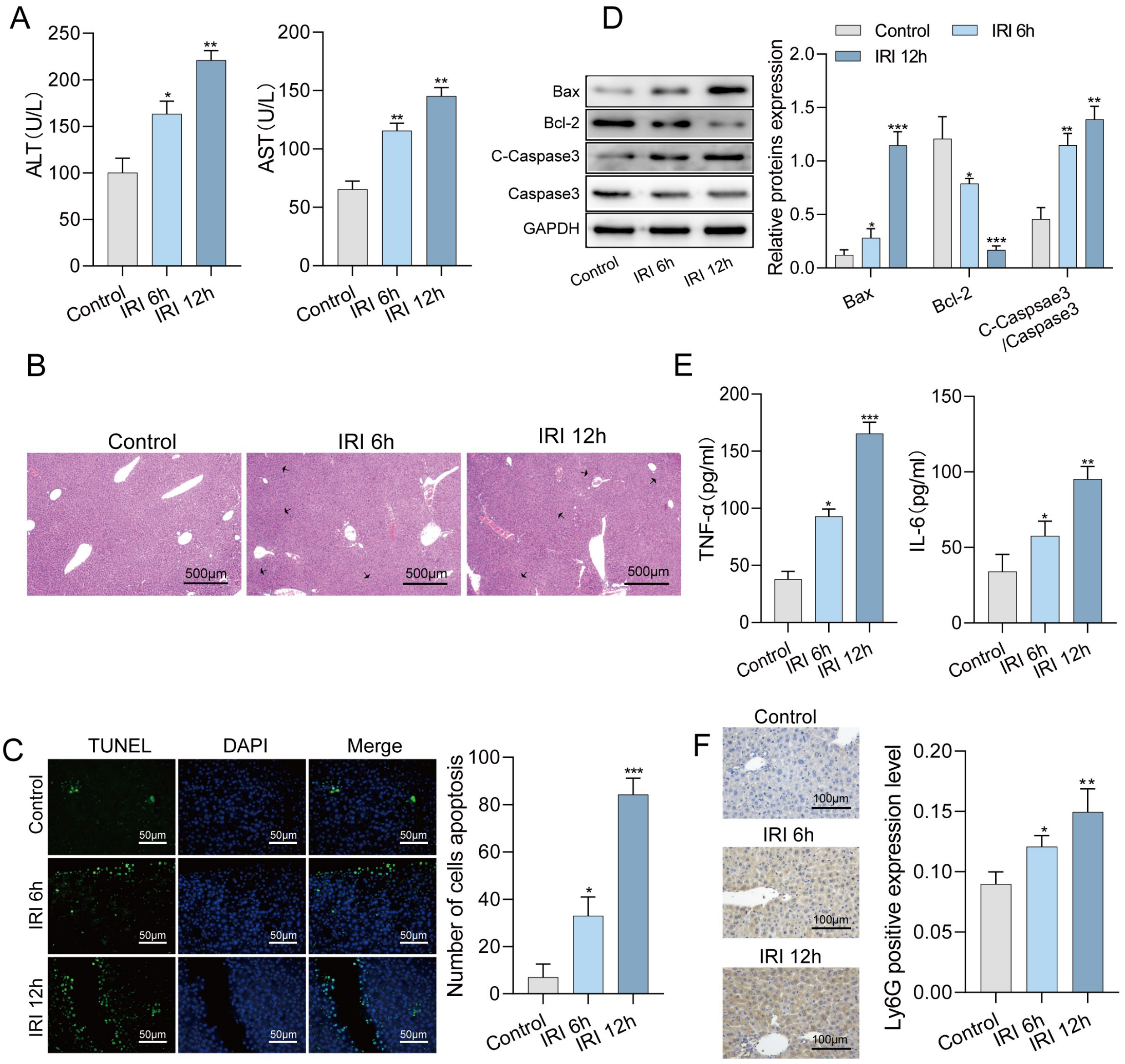

Fig. 1. Hyperlipidemia enhanced hepatic ischemia-reperfusion injury (IRI). (A) Automatic biochemical analyzer detection of serum aspartate aminotransferase (AST) and serum alanine aminotransferase (ALT) levels. (B) Hematoxylin-eosin (H&E) staining to evaluate hepatic necrosis after IRI. (C) Terminal-deoxynucleoitidyl Transferase Mediated Nick End Labeling staining to detect hepatocyte apoptosis in mice hepatic tissue. Scale bar: 50 µm. (D) Western blotting to detect the expression of Cleaved Caspase-3 (C-Caspase3), Caspase3, BCL2-Associated X, and B-cell lymphoma-2 in mouse hepatic tissue. (E) Enzyme linked immunosorbent assay detection of the expression levels of inflammatory factors Tumor necrosis factor-α and Interleukin-6 in mice serum. (F) Immunohistochemical staining to evaluate the Ly6G positive expression. All the results were presented as mean ± standard deviation (SD) (n = 3). (*$p < 0.05$, **$p < 0.01$, ***$p < 0.001$ *vs* Control group).

fusion time prolonged (Fig. 1C, $p < 0.05$). Additionally, the expression levels of the apoptosis proteins C-Caspase3 (Fig. 1D, $p < 0.01$) and Bax (Fig. 1D, $p < 0.05$) in hepatic tissue significantly increased with prolonged reperfusion time, while the expression level of the anti-apoptotic protein Bcl-2 significantly decreased (Fig. 1D, $p < 0.05$). Furthermore, ELISA detection results also demonstrated a gradual increase in the expression levels of inflammatory factors TNF-α (Fig. 1E, $p < 0.05$) and IL-6 (Fig. 1E, $p < 0.05$) with prolonged reperfusion time, compared to the control group. Importantly, the hepatic infiltration of neutrophils, assessed by immunohistochemical staining of the neutrophil-specific marker Ly6G, increased significantly at 6 and 12 h after reperfusion, compared with the control group (Fig. 1F, $p < 0.05$). These findings suggest that hyperlipidemia can exacerbate hepatic IRI, potentially due to the infiltration of a significant number of neutrophils.

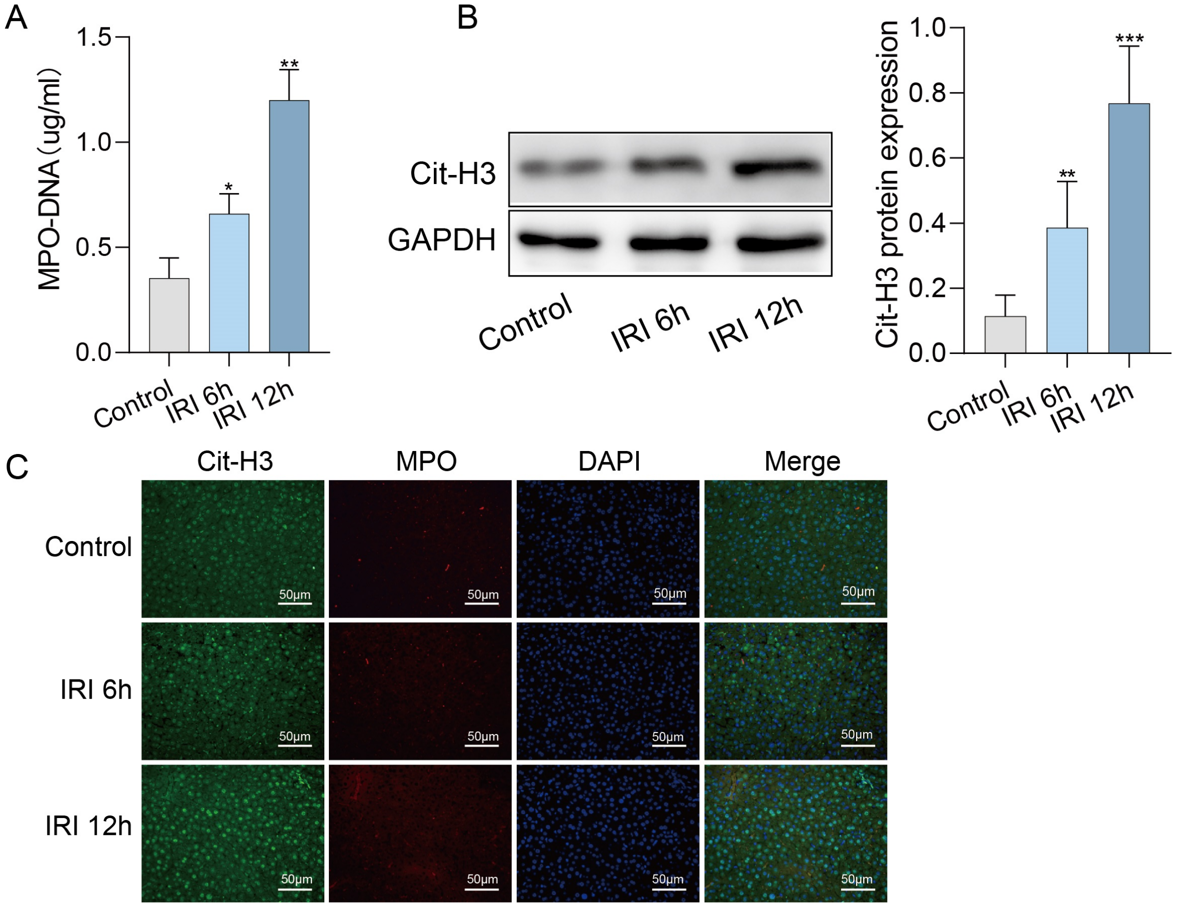

Fig. 2. Hyperlipidemia promoted the formation of neutrophil extracellular traps (NETs) in hepatic IRI. (A) ELISA detection of myeloperoxidase (MPO)-DNA complexes content. (B) Western blotting was used to detect the expression of citrullinated histone H3 (Cit-H3) in hepatic tissues. (C) Immunofluorescence was used to label Cit-H3 and MPO co-localization. Scale bar: 50 μm. All the results were presented as mean ± SD (n = 3). (*$p < 0.05$, **$p < 0.01$, ***$p < 0.001$ *vs* Control group).

Hyperlipidemia Promoted the Formation of NETs in Hepatic IRI

To investigate the formation of NETs during hepatic IRI, we initially examined the presence of NETs in mouse serum following reperfusion. The levels of MPO-DNA complexes significantly increased with longer reperfusion time compared to the control group (Fig. 2A, $p < 0.05$). Subsequently, western blot analysis revealed a significant increase in the NETs marker Cit-H3 as reperfusion time prolonged (Fig. 2B, $p < 0.01$). Furthermore, immunofluorescence staining was utilized to co-localize Cit-H3 and MPO in hepatic samples (Fig. 2C), showing a notable increase in MPO-CitH3 expression over time after reperfusion. These findings confirm that hyperlipidemia can induce the formation of NETs in hepatic IRI.

Hyperlipidemia Promoted the Formation of NETs after Hepatic IRI by the oxLDL/Mac-1 Pathway

We further explored the mechanism of NETs. Previous studies have indicated that the aggregation, activation, and release of NETs can be induced by the oxidation of LDL and the activation of the specific membrane receptor Mac-1 on macrophages [21,22]. We observed a significant increase in serum oxLDL levels with time after reperfusion (Fig. 3A, $p < 0.05$). Subsequently, immunofluorescence analysis of hepatic tissues after perfusion showed a significant increase in Mac-1 expression over time (Fig. 3B, $p < 0.05$). Furthermore, the expression level of Mac-1 protein was significantly elevated with prolonged perfusion time (Fig. 3C, $p < 0.01$). The nuclear factor kappa-B proinflammatory signaling pathway can promote the inflammatory response induced by NETs [23]. Our protein blot analysis revealed that the activation of the inflammatory NF-κB signaling pathway increased over time, as indicated by the elevated expression of p-p65, while the expression of p65 showed no significant change (Fig. 3D, $p < 0.01$). To investigate whether NETs formation was mediated by the oxLDL/Mac-1 pathway, we downregulated Mac-1 and observed a significant decrease in the content of MPO-DNA complexes (**Supplementary Fig. 1A**, $p < 0.05$) and a decrease in Cit-H3 protein expression level (**Supplementary Fig. 1B**, $p < 0.05$) in the IRI 12 h + si-Mac-1 group com-

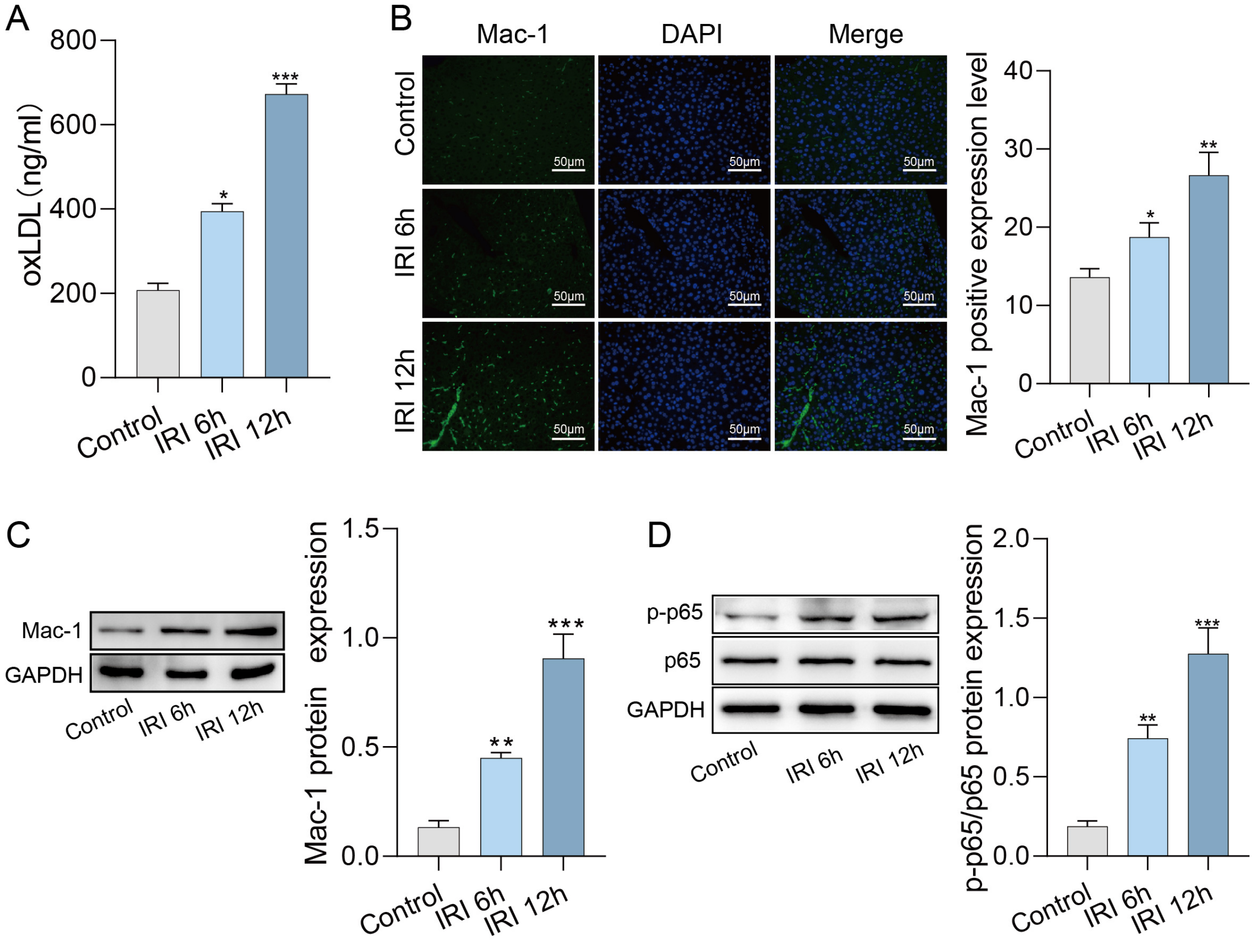

Fig. 3. Hyperlipidemia promoted the formation of NETs after hepatic IRI by the oxidized low-density lipoprotein (oxLDL)/ Macrophage-1antigen (Mac-1) pathway. (A) ELISA measurement of serum oxLDL levels. (B) Immunofluorescence staining of Mac-1 expression in hepatic tissues. Scale bar: 50 μm. (C) Western blotting analysis of Mac-1 expression in hepatic tissues. (D) Western blotting analysis of p65, phospho-nuclear factor kappa-B/p65 expression in hepatic tissues. All the results are presented as mean ± SD (n = 3). (*$p < 0.05$, **$p < 0.01$, ***$p < 0.001$ *vs* Control group).

pared to the IRI 12 h group. This suggests that NETs formation is suppressed after the downregulation of Mac-1. Additionally, we found that the downregulation of Mac-1 inhibited the activation of the NF-κB pathway, and decreased the value of p-p65/p65 (**Supplementary Fig. 1C**, $p < 0.001$) after 12 h of perfusion. Based on these results, our study suggests that hyperlipidemia induces the formation of NETs through the oxLDL/Mac-1 pathway, promoting the formation of NETs after hepatic IRI.

SIM Inhibited NETs Formation via the oxLDL/Mac-1 Pathway

To investigate the potential of SIM in reducing NETs formation via the oxLDL/Mac-1 pathway induced by hyperlipidemia, we selected the 12-hour time point after reperfusion for SIM treatment. Our findings revealed a significant decrease in Ly6G positive expression in the hepatic tissue following IRI after 12 h of SIM treatment (Fig. 4A, $p < 0.05$). Furthermore, there was a notable reduction in the levels of MPO-DNA complexes in the serum of mice (Fig. 4B, $p < 0.05$), along with a decrease in Cit-H3 protein expression, a recognized marker for NETs formation, in liver tissues (Fig. 4C,D, $p < 0.01$). Additionally, the co-localization of MPO-CitH3 in hepatic tissues was inhibited by SIM treatment (Fig. 4E). Moreover, the expression of oxLDL and Mac-1 was significantly lower after 12 h of SIM treatment compared to IRI alone (Fig. 4F,G, $p < 0.05$). To further investigate whether SIM inhibits the formation of NETs through the oxLDL/Mac-1 pathway, we overexpressed Mac-1 after SIM treatment, as shown in **Supplementary Fig. 2**. Overexpression of Mac-1 reversed the effect of SIM, significantly promoting the expression of Cit-H3 protein (**Supplementary Fig. 2A**, $p < 0.01$) and upregulating the levels of MPO-DNA complexes (**Supplementary Fig. 2B**, $p < 0.05$). In conclusion, our results strongly suggest that SIM can effectively reduce neutrophil infiltration and restrain NETs formation by the oxLDL/Mac-1 pathway.

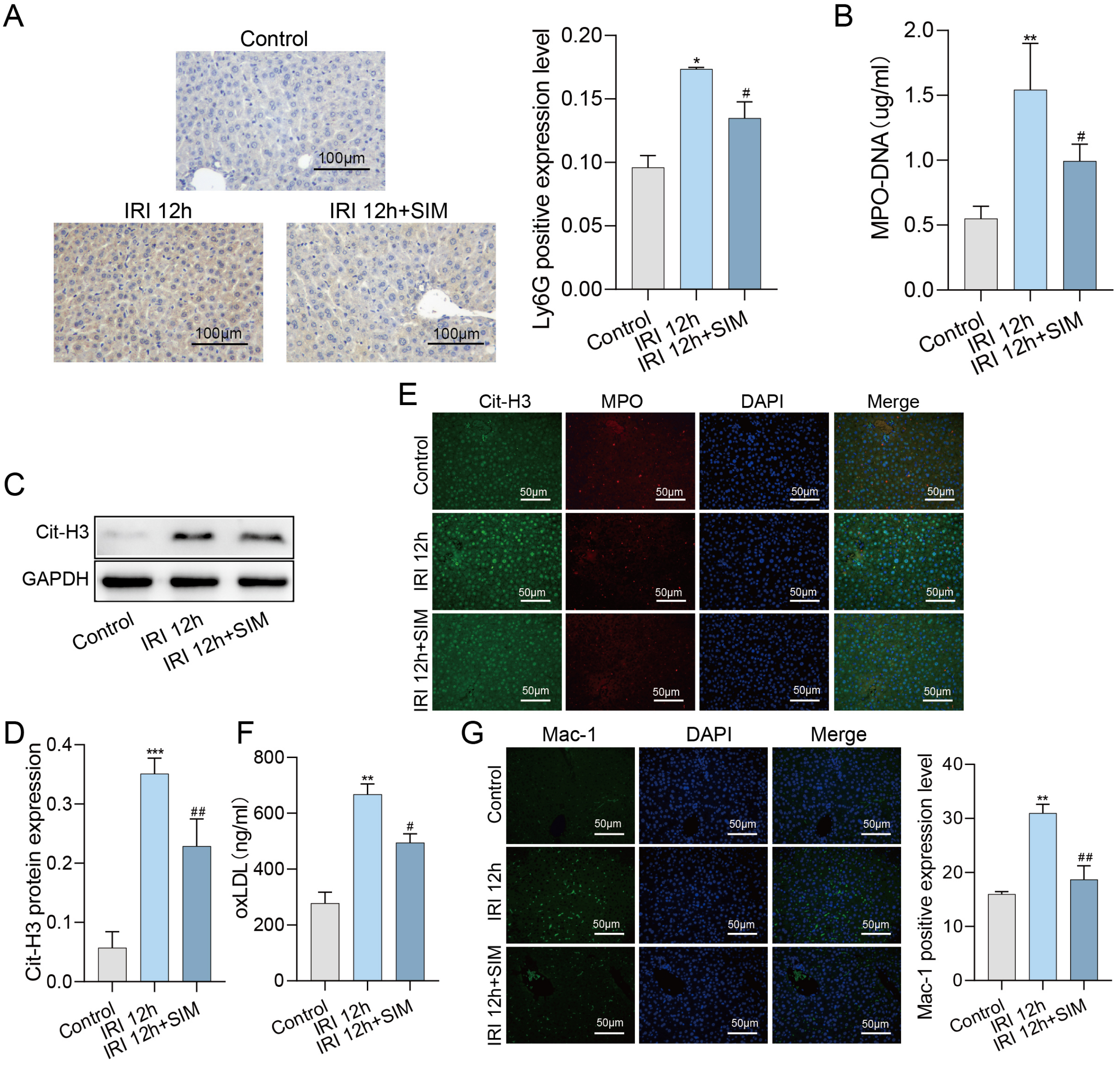

Fig. 4. Simvastatin (SIM) inhibited NETs formation via the oxLDL/Mac-1 pathway. (A) Immunohistochemistry staining of Ly6G in hepatic tissues. (B) ELISA measurement of MPO-DNA complex levels. (C,D) Western blot analysis of Cit-H3 expression in hepatic tissues. (E) Co-localization of MPO-CitH3 was assayed by immunofluorescence staining. (F) ELISA measurement of serum oxLDL levels. (G) Immunofluorescence staining of Mac-1 expression in hepatic tissues. All the results are presented as mean ± SD (n = 3). (*$p < 0.05$, **$p < 0.01$, ***$p < 0.001$ *vs* Control group, $^{\#}p < 0.05$, $^{\#\#}p < 0.01$ *vs* IRI 12 h group).

SIM Inhibited Hepatic IRI Caused by Hyperlipidemia

The results showed that SIM treatment reduced the levels of ALT (Fig. 5A, $p < 0.05$) and AST (Fig. 5A, $p < 0.01$) after 12 h of IR. It also improved the visibility of the hepatic cord, decreased the area of coagulative necrosis, and relieved hepatic tissue (black arrow) (Fig. 5B). Additionally, SIM inhibited liver cell apoptosis (Fig. 5C, $p < 0.01$), decreased the expression levels of apoptosis proteins C-Caspase3/Caspase3 (Fig. 5D, $p < 0.01$) and Bax (Fig. 5D, $p < 0.01$), and upregulated the expression of the anti-apoptotic protein Bcl-2 (Fig. 5D, $p < 0.05$). Furthermore, SIM treatment decreased the levels of TNF-α (Fig. 5E, $p < 0.05$) and IL-6 (Fig. 5E, $p < 0.05$) in liver tissues after IRI, suggesting that SIM inhibits hepatic IRI caused by hyperlipidemia.

Discussion

Hepatic IRI is an unavoidable complication during hepatic resection and transplantation surgeries. In recent decades, the increasing prevalence of hyperlipidemia has emerged as a major cause of IRI [24]. In this study, a mouse model was successfully established to simulate

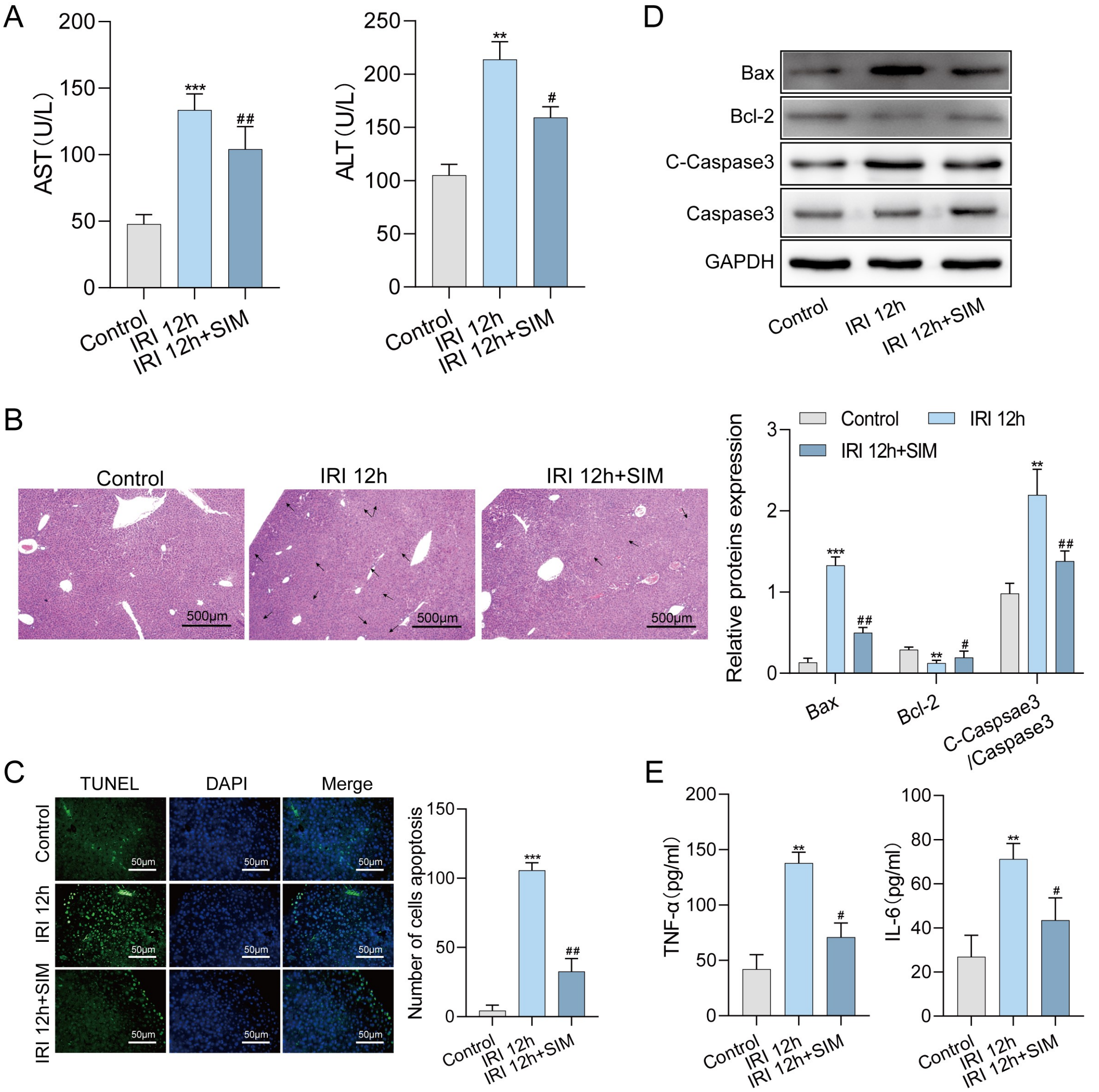

Fig. 5. SIM inhibited hepatic IRI caused by hyperlipidemia. (A) AST and ALT levels were analyzed using an automated biochemical analyzer. (B) H&E staining evaluation of hepatic tissue necrosis. (C) TUNEL staining was used to detect hepatic cell apoptosis. Scale bar: 50 μm. (D) Western blot analysis of C-Caspase3, Caspase3, Bax, and Bcl-2 expression in hepatic tissues. (E) ELISA measurement of TNF-α and IL-6 levels in serum. All the results are presented as mean ± SD (n = 3). (**$p < 0.01$, ***$p < 0.001$ *vs* Control group, $^{\#}p < 0.05$, $^{\#\#}p < 0.01$ *vs* IRI 12 h group).

hyperlipidemia-induced hepatic IRI. We observed a significant increase in hepatic damage with prolonged reperfusion time. Indicators of liver injury and inflammation, such as ALT, AST, TNF-α, and IL-6, exhibited a gradual rise in the mice's serum over time. Moreover, the area of hepatic necrosis and the number of apoptotic hepatocytes increased progressively. The expression levels of C-Caspase3 and Bax, proteins associated with apoptosis, also increased, while the anti-apoptotic protein Bcl2 increased with prolonged reperfusion time.

NETs are a novel mechanism discovered in 2004, involving the capture and killing of infectious pathogens by neutrophils. Over the past decade, research has increasingly focused on the occurrence and development of NETs in non-infectious diseases, including cancer [25], autoimmune diseases [26], thrombosis [27], and sterile inflammatory tissue damage [28]. In particular, NETs play a key role in sterile inflammatory tissue damage, specifically hepatic IRI. Studies have shown that after hepatic IRI occurs, NETs and their important components, such as MPO, histones, and NE, can serve as damage-associated molecular patterns (DAMPs), initiating and amplifying inflammatory responses and activating the immune system. While causing damage to hepatic parenchymal cells, they exert cytotoxic effects on the liver's vascular endothelium, leading to widespread hepatocyte necrosis, cell apoptosis, and autoimmune liver diseases [29]. However, the specific mechanism of NETs formation in hepatic IRI is still unclear. Therefore, our study intends to further explore the molecular mechanism of NETs formation mediated by hyperlipidemia in hepatic IRI. During hepatic IRI, hyperlipidemia-mediated oxidative stress leads to the oxidation of LDL to oxLDL. On the one hand, we consider that intracellular oxLDL directly induces the production of NETs through the TLR-MAPK pathway, stimulating inflammatory responses and exacerbating hepatic IRI [30]. On the other hand, oxLDL can stimulate platelets to enhance the infiltration of neutrophils [31], and it is known that platelets can induce the formation of NETs on activated neutrophils by activating Mac-1 [32]. We hypothesized that oxLDL in the body may stimulate the expression of Mac-1, leading to the formation of NETs. As anticipated, our experimental results demonstrated that the level of Cit-H3, a marker protein of NETs, and the quantity of MPO-DNA complexes in the serum gradually increased over time after reperfusion. Importantly, we also observed elevated expression levels of oxLDL and Mac-1. These findings suggest that hyperlipidemia may facilitate the generation of NETs through the oxLDL/Mac-1 pathway.

SIM is a lipid-lowering drug of the statin class, with significant therapeutic effects in controlling cholesterol levels in the blood and preventing cardiovascular diseases [33]. However, the treatment mechanism of SIM in hepatic IRI is not fully understood. This study found that SIM decreased the levels of AST and ALT in the serum, reduced the aggregation of neutrophils, decreased hepatic cell apoptosis, improved hepatic function, and alleviated hepatic IRI. Researches have confirmed that SIM can reduce neutrophil infiltration during IRI [18,34]. Furthermore, this study aimed to investigate whether SIM could alleviate hyperlipidemia-mediated hepatic IRI by inhibiting the formation of NETs through the oxLDL/Mac-1 pathway, as suggested by the findings in Figs. 2,3. It was hypothesized that SIM intervention might hinder the generation of NETs by targeting the oxLDL/Mac-1 pathway. As expected, the research observed a decline in MPO-DNA levels in the serum and a reduction in Cit-H3 expression, indicating that SIM effectively suppressed the formation of NETs. Moreover, the study detected a significant inhibition of oxLDL and Mac-1 expression following SIM treatment. These results suggest that simvastatin alleviates hyperlipidemia-mediated liver IRI by suppressing the formation of NETs through the oxLDL/Mac-1 pathway. However, this study has several limitations. First, it did not investigate the dose effect of SIM and only used one dose (5 mg/kg), which cannot determine the optimal therapeutic dose and time window of SIM. Future studies need to include different doses and time points of SIM treatment to verify the best intervention strategy. Second, the study did not evaluate the safety and toxicity of SIM, and cannot rule out the adverse effects of SIM on other organs or systems. Lastly, the study did not explore the effects of SIM on other factors related to hepatic IRI, such as liver metabolism, liver fibrosis, and liver regeneration.

Conclusions

In summary, our study demonstrated that the use of simvastatin alleviates hyperlipidemia-mediated hepatic IRI. The protective mechanism of SIM against hepatic IRI may be mediated through the regulation of the oxLDL/Mac-1 pathway, inhibition of NETs formation, and inflammation response. Our research strongly supports the inhibitory effect of SIM on NETs formation during hepatic IRI, and its potential as a viable strategy for protecting liver function during hepatic surgeries.

Availability of Data and Materials

For data and materials availability, please contact the corresponding author.

Author Contributions

SW, ZL and XC designed the research study. ZL and YC provided help and advice on the animal experiments. SW and ZL collected and integrated the data. KD and DH analyzed the data. XC performed the research. All authors contributed to editorial changes in the manuscript. All authors read and approved the final manuscript. All authors have participated sufficiently in the work and agreed to be accountable for all aspects of the work.

Ethics Approval and Consent to Participate

All experiments were approved by the Animal Ethics Committee of the Guangzhou Seyotin Biotechnology Co., Ltd. (SYT2023010).

Acknowledgment

Not applicable.

Funding

This research was supported by the Shenzhen Basic Research Project (No. JCYJ20190809101413443), Shenzhen Nanshan District science and technology plan key project (No. 2020005), Hospital project of Union Shenzhen Hospital of Huazhong University of Science and Technology (No.YN2022020), Shenzhen Nanshan District Health System Science and Technology Major Project (No. NSZD2023045, No. NSZD2023001).

Conflict of Interest

The authors declare no conflict of interest.

Supplementary Material

Supplementary material associated with this article can be found, in the online version, at https://doi.org/10.24976/Discov.Med.202436187.158.

References

[1] Yan HF, Tuo QZ, Yin QZ, Lei P. The pathological role of ferroptosis in ischemia/reperfusion-related injury. Zoological Research. 2020; 41: 220–230.

[2] Ni X, Wu X, Zhu XX, Li JH, Yin XY, Lu L. Carabin Deficiency Aggravates Hepatic Ischemia-Reperfusion Injury Through Promoting Neutrophil Trafficking *via* Ras and Calcineurin Signaling. Frontiers in Immunology. 2022; 13: 773291.

[3] Hirao H, Nakamura K, Kupiec-Weglinski JW. Liver ischaemia-reperfusion injury: a new understanding of the role of innate immunity. Nature Reviews. Gastroenterology & Hepatology. 2022; 19: 239–256.

[4] Han D, Wei J, Zhang R, Ma W, Shen C, Feng Y, *et al*. Hydroxysafflor yellow A alleviates myocardial ischemia/reperfusion in hyperlipidemic animals through the suppression of TLR4 signaling. Scientific Reports. 2016; 6: 35319.

[5] Tung YT, Wu CH, Chen WC, Pan CH, Chen YW, Tsao SP, *et al*. *Ascophyllum nodosum* and *Fucus vesiculosus* Extracts Improved Lipid Metabolism and Inflammation in High-Energy Diet-Induced Hyperlipidemia Rats. Nutrients. 2022; 14: 4665.

[6] Sato K, Yao T, Fujimura T, Murayama K, Okumura K, Hagiwara N, *et al*. Oxidative stress-responsive apoptosis-inducing protein in patients with heterozygous familial hypercholesterolemia. Heart and Vessels. 2021; 36: 1923–1932.

[7] Li J, Yin L, Chen S, Li Z, Ding J, Wu J, *et al*. The perspectives of NETosis on the progression of obesity and obesity-related diseases: mechanisms and applications. Frontiers in Cell and Developmental Biology. 2023; 11: 1221361.

[8] Liu Y, Qin X, Lei Z, Chai H, Huang Z, Wu Z. Tetramethylpyrazine inhibits neutrophil extracellular traps formation and alleviates hepatic ischemia/reperfusion injury in rat liver transplantation. Experimental Cell Research. 2021; 406: 112719.

[9] Zhu C, Shi S, Jiang P, Huang X, Zhao J, Jin Y, *et al*. Curcumin Alleviates Hepatic Ischemia-Reperfusion Injury by Inhibiting Neutrophil Extracellular Traps Formation. Journal of Investigative Surgery: the Official Journal of the Academy of Surgical Research. 2023; 36: 2164813.

[10] Honda M, Kubes P. Neutrophils and neutrophil extracellular traps in the liver and gastrointestinal system. Nature Reviews. Gastroenterology & Hepatology. 2018; 15: 206–221.

[11] Gocho T, Mori H, Islam MM, Maruchi Y, Takenaka N, Tomino A, *et al*. Removal of Circulating Neutrophil Extracellular Trap Components With an Immobilized Polymyxin B Filter: A Preliminary Study. Shock (Augusta, Ga.). 2020; 54: 44–49.

[12] Vorobjeva NV, Chernyak BV. NETosis: Molecular Mechanisms, Role in Physiology and Pathology. Biochemistry. Biokhimiia. 2020; 85: 1178–1190.

[13] Sule G, Kelley WJ, Gockman K, Yalavarthi S, Vreede AP, Banka AL, *et al*. Increased Adhesive Potential of Antiphospholipid Syndrome Neutrophils Mediated by $\beta 2$ Integrin Mac-1. Arthritis & Rheumatology (Hoboken, N.J.). 2020; 72: 114–124.

[14] Behnen M, Leschczyk C, Möller S, Batel T, Klinger M, Solbach W, *et al*. Immobilized immune complexes induce neutrophil extracellular trap release by human neutrophil granulocytes via FcγRIIIB and Mac-1. Journal of Immunology (Baltimore, Md.: 1950). 2014; 193: 1954–1965.

[15] Liu Z, Lai CH, Zhang X, Luo J, Huang X, Qi X, *et al*. Simvastatin ameliorates total liver ischemia/reperfusion injury via KLF2-mediated mechanism in rats. Clinics and Research in Hepatology and Gastroenterology. 2019; 43: 171–178.

[16] Wei T, Li J, Fu G, Zhao H, Huang C, Zhu X, *et al*. Simvastatin Improves Myocardial Ischemia Reperfusion Injury through KLF-Regulated Alleviation of Inflammation. Disease Markers. 2022; 2022: 7878602.

[17] Yan Y, Lv X, Ma J, Hong G, Li S, Shen J, *et al*. Simvastatin Alleviates Intestinal Ischemia/Reperfusion Injury by Modulating Omi/HtrA2 Signaling Pathways. Transplantation Proceedings. 2019; 51: 2798–2807.

[18] Cowled PA, Khanna A, Laws PE, Field JBF, Fitridge RA. Simvastatin plus nitric oxide synthase inhibition modulates remote organ damage following skeletal muscle ischemia-reperfusion injury. Journal of Investigative Surgery: the Official Journal of the Academy of Surgical Research. 2008; 21: 119–126.

[19] Li J, Wu H, Liu Y, Yang L. High fat diet induced obesity model using four strainsof mice: Kunming, C57BL/6, BALB/c and ICR. Experimental Animals. 2020; 69: 326–335.

[20] Zhao Y, Feng Q, Huang Z, Li W, Chen B, Jiang L, *et al*. Simvastatin inhibits inflammation in ischemia-reperfusion injury. Inflammation. 2014; 37: 1865–1875.

[21] Huang C, Han J, Wu Y, Li S, Wang Q, Lin W, *et al*. Exosomal MALAT1 derived from oxidized low-density lipoprotein-treated endothelial cells promotes M2 macrophage polarization. Molecular Medicine Reports. 2018; 18: 509–515.

[22] McDonald B, Davis RP, Kim SJ, Tse M, Esmon CT, Kolaczkowska E, *et al*. Platelets and neutrophil extracellular traps collaborate to promote intravascular coagulation during sepsis in mice. Blood. 2017; 129: 1357–1367.

[23] Liu D, Yang P, Gao M, Yu T, Shi Y, Zhang M, *et al*. NLRP3 activation induced by neutrophil extracellular traps sustains inflammatory response in the diabetic wound. Clinical Science (London, England: 1979). 2019; 133: 565–582.

[24] Du H, He Y, Zhu J, Zhou H, Shao C, Yang J, *et al*. Danhong injection alleviates cerebral ischemia-reperfusion injury by inhibiting mitochondria-dependent apoptosis pathway and improving mitochondrial function in hyperlipidemia rats. Biomedicine & Pharmacotherapy. 2023; 157: 114075.

[25] Cristinziano L, Modestino L, Antonelli A, Marone G, Simon HU, Varricchi G, *et al*. Neutrophil extracellular traps in cancer. Seminars in Cancer Biology. 2022; 79: 91–104.

[26] Fousert E, Toes R, Desai J. Neutrophil Extracellular Traps (NETs) Take the Central Stage in Driving Autoimmune Responses. Cells. 2020; 9: 915.

[27] Thakur M, Junho CVC, Bernhard SM, Schindewolf M, Noels H, Döring Y. NETs-Induced Thrombosis Impacts on Cardiovascular and Chronic Kidney Disease. Circulation Research. 2023; 132: 933–949.

[28] Münzer P, Negro R, Fukui S, di Meglio L, Aymonnier K, Chu L, *et al*. NLRP3 Inflammasome Assembly in Neutrophils Is Supported by PAD4 and Promotes NETosis Under Sterile Conditions. Frontiers in Immunology. 2021; 12: 683803.

[29] Yazdani HO, Chen HW, Tohme S, Tai S, van der Windt DJ, Loughran P, *et al*. IL-33 exacerbates liver sterile inflammation by amplifying neutrophil extracellular trap formation. Journal of Hepatology. 2018; 68: 130–139.

[30] Awasthi D, Nagarkoti S, Kumar A, Dubey M, Singh AK, Pathak P, *et al*. Oxidized LDL induced extracellular trap formation in human neutrophils via TLR-PKC-IRAK-MAPK and NADPH-oxidase activation. Free Radical Biology & Medicine. 2016; 93: 190–203.

[31] Badrnya S, Butler LM, Söderberg-Naucler C, Volf I, Assinger A. Platelets directly enhance neutrophil transmigration in response to oxidised low-density lipoprotein. Thrombosis and Haemostasis. 2012; 108: 719–729.
[32] Pulavendran S, Rudd JM, Maram P, Thomas PG, Akhilesh R, Malayer JR, *et al*. Combination Therapy Targeting Platelet Activation and Virus Replication Protects Mice against Lethal Influenza Pneumonia. American Journal of Respiratory Cell and Molecular Biology. 2019; 61: 689–701.
[33] Hodkinson A, Tsimpida D, Kontopantelis E, Rutter MK, Mamas MA, Panagioti M. Comparative effectiveness of statins on non-high density lipoprotein cholesterol in people with diabetes and at risk of cardiovascular disease: systematic review and network meta-analysis. BMJ (Clinical Research Ed.). 2022; 376: e067731.
[34] Cowled PA, Khanna A, Laws PE, Field JBF, Varelias A, Fitridge RA. Statins inhibit neutrophil infiltration in skeletal muscle reperfusion injury. The Journal of Surgical Research. 2007; 141: 267–276.